National University of Science and Technology
POLITEHNICA Bucharest
Doctoral School of Applied Sciences
Department: Physics
Field: Exact Sciences, Physics

DOCTORAL THESIS

-Summary-

OPTICAL SENSORS FOR SECURITY IN CONTAMINATED ENVIRONMENTS

PhD Candidate:
Ing. Răzvan – Marian MIHALCEA

PhD Supervisor:
Prof. Univ. Dr. Niculae PUȘCAȘ

Bucharest
2026

TABLE OF CONTENTS

CHAPTER 1. BRIEF HISTORY AND RELEVANCE OF RESEARCH 3

1.1 HISTORICAL BACKGROUND 3

CHAPTER 2. FABRICATION OF OPTICAL FIBERS AND FIBER OPTIC SENSORS 4

2.1 CLASSIFICATION OF OPTICAL FIBERS AND FIBER OPTIC SENSORS 4

2.1.1 TYPES OF OPTICAL FIBERS 4

2.1.2 OPTICAL FIBER MANUFACTURING METHODS 4

2.2 TYPES OF OPTICAL FIBER SENSORS AND THEIR FABRICATION 5

2.2.1 CLASSIFICATION OF OPTICAL FIBER SENSORS 5

2.2.2 FABRICATION OF OPTICAL FIBER SENSORS 5

CHAPTER 3. FIBER OPTIC SENSORS IN IONIZING RADIATION ENVIRONMENTS 6

3.1 EFFECTS OF RADIATION ON OPTICAL FIBERS AND FIBER OPTIC SENSORS 6

3.1.1 EFFECT OF GAMMA RADIATION ON FIBER OPTIC SENSORS 7

3.1.2 EFECTUL RADIAȚIEI CU PROTONI ȘI NEUTRONI ASUPRA SENZORILOR PE FIBRĂ OPTICĂ 9

3.1.3 EFFECT OF PROTON AND NEUTRON RADIATION ON FIBER OPTIC SENSORS 9

CHAPTER 4. OWN CONTRIBUTIONS IN THE FIELD OF IONIZING RADIATION INTERACTION WITH FIBER OPTIC SENSORS 10

4.1 LABORATORY-LEVEL CHARACTERIZATION OF OPTICAL COMPONENTS 10

4.1.1 LABORATORY CHARACTERIZATION AND CALIBRATION INFRASTRUCTURE 11

4.2 OWN CONTRIBUTIONS TO THE EXPERIMENTAL AND THEORETICAL DEVELOPMENT OF THE RESEARCH 11

4.2.1 NEW METHODS AND SETUPS FOR THE CHARACTERIZATION OF FIBER OPTIC SENSORS PLACED IN A GAMMA RADIATION FIELD 12

4.2.2 STUDY ON THE EFFECTS ON FBG-TYPE FIBER SENSORS INSCRIBED USING A FEMTOSECOND LASER, EXPOSED TO DIFFERENT TYPES OF RADIATION SUCH AS GAMMA RAYS AND ELECTRONS. 13

4.2.3 STUDY ON THE IMPACT OF GAMMA RADIATION ON LPG-TYPE SENSORS. 15

4.2.4 INVESTIGATION OF THE INTERACTION OF RADIATION WITH PLASTIC FIBERS 16

4.2.5 EVALUATION OF THE EFFECTS OF DIFFERENT TYPES OF RADIATION ON RADIATION-RESISTANT FIBERS 18

4.2.6 EFFECTS OF GAMMA RADIATION ON LPG SENSORS AND ON THE THIN FILMS DEPOSITED OVER THEM 20

4.2.7 IMPACT OF A BEAM OF ACCELERATED ELECTRONS ON LPG SENSORS FABRICATED IN DIFFERENT FIBERS 21

CHAPTER 5. CONCLUSIONS 24

5.1 GENERAL CONCLUSIONS 24

5.2 CONCLUSIONS AND OWN CONTRIBUTIONS 25

5.3 FUTURE RESEARCH DIRECTIONS 26

CHAPTER 6. REFERENCES 27

CHAPTER 1. BRIEF HISTORY AND RELEVANCE OF RESEARCH

1.1 HISTORICAL BACKGROUND

Optical sensors emerged as a necessity for different communities to communicate rapidly. At the end of the 18th century, sending messages from one point to another could take hours, days, or even weeks using conventional methods. In 1792, the French inventor Claude Chappe revolutionized the communication system by inventing the optical telegraph. In April 1794, the first line connecting Paris and Lille was inaugurated, stretching over 190 km. In 1854, the English physicist John Tyndall demonstrated that light could use a water jet as a guiding medium, even if it was curved. By creating a zig-zag path inside the stream, he discovered the effect of total internal reflection [1], marking the first documented research confirming guided light transmission and the fact that light could "bend.". In 1880, Alexander Graham Bell, in collaboration with Charles Sumner Tainter, invented the photophone, as published in the American Journal of Science [2]. The year 1930 was marked by Heinrich Lamm, who used a fiber bundle to transmit the first image through optical fibers. From the mid-20th century, optical fibers began to enter different fields and applications after Van Heel in 1954 coated a fiber rod with a transparent cladding of lower refractive index, which significantly improved its guiding properties. In 1960, Charles K. Kao, together with his colleagues, collected fiber samples from various manufacturers. They realized that the power losses in optical fibers used up to that time were largely due to impurities in the glass from which the fibers were fabricated [3]. Only a few years later, these losses were reduced to 20 dB/km. In 2009, Charles K. Kao was awarded the Nobel Prize in Physics for his "groundbreaking achievements concerning the transmission of light in fibers for optical communication," and he is regarded as the "Father of Optical Fibers". The use of fibers in telecommunications [4] is due to their unique properties, such as: low optical nonlinearity, wide bandwidth, low transmission losses, high optical damage threshold, resistance to high temperatures, immunity to electricity and magnetic fields, mechanical strength, slow material aging, small dimensions, and resistance to weathering. At present, optical fibers dominate the telecommunications industry, providing the backbone connections between main servers across continents. The longest optical fiber link, called FLAG (Fibre-optic Link Around the Globe), stretches approximately 28,000 km. Research laboratories worldwide continue to improve fiber technologies, achieving new records in data transmission. In 2023, speeds of up to 1.7 Pb/s were reported [5], and in 2024, a speed of 402 Tbps was reached in an experiment carried out by the National Institute of Information and Communications Technology (NICT).

CHAPTER 2. FABRICATION OF OPTICAL FIBERS AND FIBER OPTIC SENSORS

2.1 CLASSIFICATION OF OPTICAL FIBERS AND FIBER OPTIC SENSORS

2.1.1 Types of Optical Fibers

An optical fiber is a flexible waveguide, consisting of a core—generally made of glass—and a cladding. It has the ability to transmit an optical beam over long distances with very low optical losses. The main physical phenomenon underlying the transport of photons through the optical fiber is total internal reflection [1]. For total internal reflection to occur, the angle of incidence must be greater than the critical angle, as shown in the following relation.

$$(\sin^{-1} (n_{cl}/n_{cl}))$$

Another important criterion for fulfilling the condition of total internal reflection is the angle at which the light ray from the external medium enters the fiber core. This angle of incidence must be smaller than the numerical aperture (NA), defined by the following relation:

$$(NA) = n_a sin\alpha_m = (n_1^2 - n_2^2)^{1/2} = 2n\Delta n$$

where

$$\Delta n = (n_1 - n_2) \text{ iar } n = (n_1 + n_2)/2.$$

Optical fibers are divided into two main categories:

- Single-mode fibers with a very narrow core of 8 µm–10 µm: allow the propagation of photons through a single mode and are used for long-distance communications, offering a large bandwidth.

- Multimode fibers with a core of 50 µm–62.5 µm: allow the simultaneous propagation of multiple modes, present high dispersion, and are used for short-distance applications (LAN, data centers).

2.1.2 Optical Fiber Manufacturing Methods

The methods of manufacturing optical fibers have evolved over the years with the discovery of new technologies. These advancements have enabled the improvement of fiber quality and production processes. The main methods include:

- The Crucible Method, in which the materials that compose the fiber are placed in a silicon or platinum crucible in the form of powders or rods and are heated.
- Vapor Deposition Method, used when the melting temperature of the materials that make up the optical fiber is too high for the crucible method. There are three types of vapor deposition for optical fibers: Inside Vapor Deposition (IVD), Outside Vapor Deposition (OVD), and Vapor Axial Deposition (VAD).

2.2 TYPES OF OPTICAL FIBER SENSORS AND THEIR FABRICATION

2.2.1 Classification of Optical Fiber Sensors

Optical fiber sensors are devices that transform the physical values of a detected phenomenon—such as pressure, temperature, humidity, mechanical stress, radiation, and others—into changes of a light beam, which can then be converted into electrical signals to be interpreted by a measuring and control device. Optical fiber sensors can be classified in several ways, depending on different criteria:

By the location of the sensitive element: intrinsic sensors and extrinsic sensors.

By the operating principle: intensity-based, phase-based, frequency/spectrum-based, and polarization-based sensors.

By the physical quantity measured: temperature sensors, pressure sensors, vibration/acoustic sensors, strain/stress sensors, and current/electromagnetic field sensors.

By detection method: point sensors or distributed sensors.

2.2.2 Fabrication of Optical Fiber Sensors

The fabrication of optical fiber sensors has been of major interest since the creation of the first Fiber Bragg Grating (FBG) sensor by Ken Hill [6] in 1978. The most common, important, and extensively studied optical fiber sensors are fiber Bragg grating (FBG) sensors.

2.2.2.1 Operating Principle of FBG Sensors.

Within an optical fiber, Bragg grating optical filters are inscribed, which reflect a narrow band of wavelengths from the entire spectrum transmitted through the fiber, while the rest of the spectrum passes without modification [7]. The change in the refractive index and the periodicity with which it varies are described by Bragg's equation:

$$\lambda_B = 2 \cdot n_{eff} \cdot \Lambda_B$$

Where n_{eff} represents the effective refractive index of the core, and Λ_B is the grating period. The Bragg wavelength corresponding to the above equation is reflected, while the rest of the spectrum propagates through the Bragg grating without experiencing interference or attenuation.

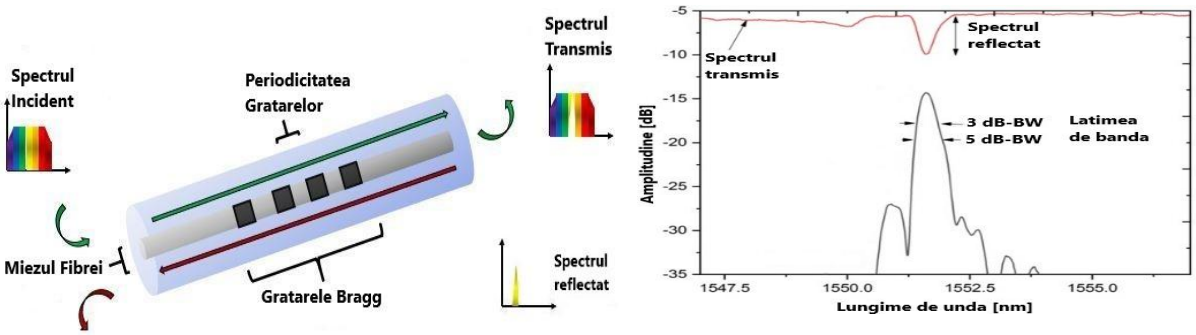


Fig.1. Block diagram of an FBG-type sensor and its graphical representation

The main characteristics of FBG-type sensors are: reflectivity (R), the central wavelength called the Bragg wavelength (λ_B), and the bandwidth. The sensor's reflectivity can be calculated using the formula:

$$R_{max} = tanh^2(kL) = tanh^2\left(\frac{\pi \Delta n_{mod} \eta L}{\lambda_B}\right)$$

where k is the coupling coefficient, L is the length of the Bragg grating filter, Δn_mod represents the change in the refractive index, and η represents the mode overlap parameter between the fiber cladding and its core.

The modulation of the refractive index (Δn_mod) induced by laser radiation is given by the equation:

$$\Delta n_{mod} = \frac{\lambda_B}{2\pi\eta L} ln\left[\frac{1+\sqrt{R}}{1-\sqrt{R}}\right]$$

the parameters η and k can be determined from the expressions:

$$\eta = \frac{\pi^2 d^2 NA^2}{\lambda_B^2 + \pi^2 d^2 NA^2}$$

$$kL = \frac{\pi}{2}$$

where d is the core diameter, and NA is the numerical aperture of the fiber used.

CHAPTER 3. FIBER OPTIC SENSORS IN IONIZING RADIATION ENVIRONMENTS

The use of fiber-optic sensors in contaminated or radioactive environments has become commonplace today. These types of sensors are employed in critical infrastructures such as research nuclear reactors, particle accelerators, industrial irradiators, space-related infrastructures, and other strategically important facilities.

3.1 Effects of Radiation on Optical Fibers and Fiber Optic Sensors

It has been demonstrated that the manufacturing parameters of optical fibers and the sensors inscribed in them directly influence their behavior when operating in ionizing radiation environments.

The fiber cladding is also important regarding exposure to ionizing radiation. In most cases, the fiber cladding is removed to create new gratings, after which the fiber core is recoated with a protective layer. During recoating, the fiber cladding is exposed to UV light to solidify more quickly, which affects the sensor's radiation sensitivity [8]. Due to these phenomena, various studies have been conducted aiming to improve the radiation tolerance of fiber optic sensors for different applications [9], [10], [11].

3.1.1 Effect of Gamma Radiation on Fiber Optic Sensors

Many studies in the field of fiber optic sensors in radiation environments are conducted using gamma radiation as the primary irradiation source. Real-time recording of caracteristicilor the sensors' spectra during irradiation has drawn researchers' attention to the temporary effects on fiber optic sensors during an irradiation session. To prevent these temporary effects, various experimental configurations have been studied and reported in the literature. [12], [13].

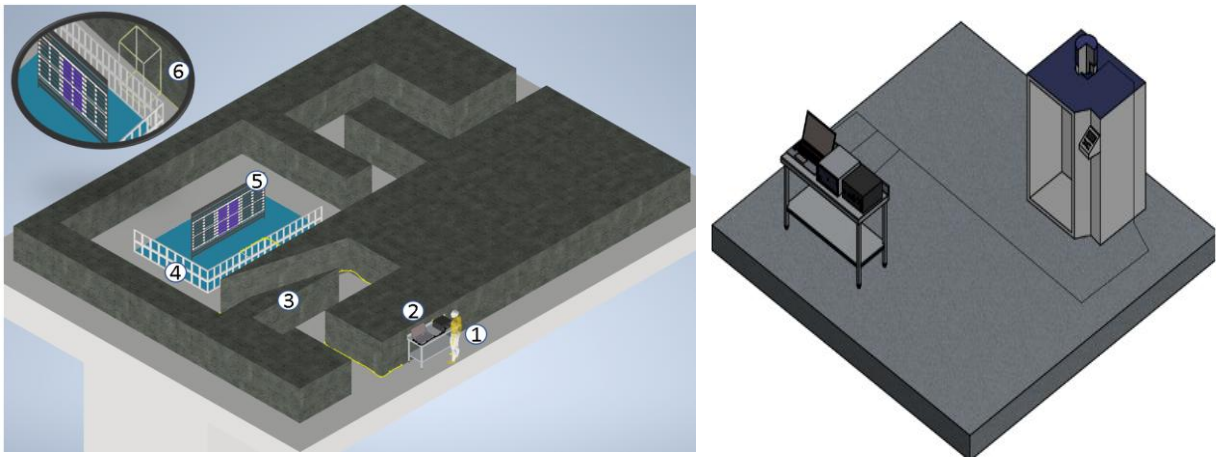


Fig.2. IRASM 3D Representation of Two Industrial Irradiation Facilities at IFIN-HH IRASM

Figure 2 shows a 3D representation of an industrial irradiator and a research irradiator at the "Horia Hulubei" National Institute for Research and Development in Physics and Nuclear Engineering (IFIN-HH).
Both irradiators have the same elements, but they are arranged differently. For this reason, only the areas of interest for the industrial irradiator are shown: the operator's position (1) outside the irradiation zone, the measurement and control instruments, the access corridor to the irradiation chamber (3), the irradiation chamber (4), the Co-60 source (5), and any elements to be irradiated placed in front of the source (6).

Gamma Beam Irradiation Experiments

One of the first studies addressing the interaction between gamma radiation and FBG-type sensors was published in November 1994 by P. Niay [9]. The authors investigated the behavior of FBG sensors inscribed in germanium-silicon fibers exposed to total radiation doses of up to 10 kGy, with dose rates ranging from 10 Gy/h to 130 Gy/h.
Another reference study was conducted in 1999, with T.A. Gusarov as the lead author [14], and this research was continued in 2017 in [15]. The authors studied the effects of radiation on the temperature sensitivity of seven FBG-type sensors inscribed in silicon fibers doped with 10% germanium.

To better understand the effects of radiation on fiber optic sensors, Table 3 was created, showing the response of each fiber optic sensor depending on the material of the fiber, the type of radiation it was exposed to, the dopants present in the core/cladding, and the total accumulated dose.

Table 1. Effects of gamma radiation on FBG sensors inscribed in optical fibers, depending on the fibers used for their inscription and the sensor fabrication methods.

Type of FBG	Type of radiation	Fiber material	Cladding dopants	Core dopants	Fabrication method	Total Accumulated dose [kGy]	Wavelenght shift [pm]	REF.
Type I	Gamma	Glass	F, P	Ge	Laser UV	10	0.1	[9]
			B, P	Ge				
			F, P	Ge, Al				
			F	Ge, F				
Type I	Gamma	Glass	-	Ge	Phase mask	1000	25	[14]
Type I, II	Gamma	Glass	-	-	Laser KrF; Hydrogen treatment	100	125	[16]
			Fără	-			120	
			Fără	-			100	
			Fără	-			80	
			GeO_2, F	GeO_2			160	
			GeO_2, F	GeO_2			80	
			Fără	GeO_2			110	
			Fără	-			160	
			Fără	-			125	
			P_2O_5, F	Al_2O_3, P_2O_5,F			50	
			P_2O_5	Al_2O_3, P_2O_5 CeO_2	Excimer laser		50	
			P_2O_5	GeO_2, CeO_2			110	
-	Gamma	Glass	F	None	SMF doped with F	200	2-20	[17]
					Phase mask		5-20	
Type I	Gamma	Glass	F	None	Phase mask	250	9 - 30	[18]
							3 -16	
Type I	Gamma	Glass	Ge	None	DTG, FBG*	33.9	~ 20	[19]
Type II	Gamma	Polymer	-	CYTOP	Plan to plan	120	~1200	[20]
-	Gamma	Glass	B	Ge	Phase mask laser KrF	22.85	11	[21]

3.1.2 Efectul radiației cu protoni și neutroni asupra senzorilor pe fibră optică

Mediul spațial este caracterizat în principal de o varietate de radiații ionizante, fotoni, protoni, electroni sau ioni grei. Prin multitudinea de studii efectuate în ultimii ani [97], [98], [99], s-a ajuns la concluzia că răspunsul la radiație furnizat de fibra optică sau dispozitivele bazate pe fibră este influențat în principal de sensibilitatea la doza totală de ionizare [100].

Pentru o vedere mai amplă asupra subiectului, informații din acest capitol vor fi prezentate în tabelul 4 din următorul capitol.

3.1.3 Effect of Proton and Neutron Radiation on Fiber Optic Sensors

Based on applications, and also considering the effects of an electron beam on FBG-type sensors inscribed in radiation-resistant optical fibers, the work of D. Sporea [22] is one of the few [23] that addresses this subject. The authors identified the need to remotely monitor an electron beam in real time.
The following table summarizes data on the interaction between different types of radiation and multiple optical fibers in which various sensors are inscribed.
Table 2. Effects of ionizing radiation on sensors inscribed in different types of optical fibers using various methods.

Type of FBG	Type of radiation	Fiber material	Cladding dopants	Core dopants	Fabrication method	Total accumulated dose [kGy]	Wavelength modification [pm]	Ref.
-	Protons	Glass	-	Ge	Laser Ar	100	20	[24]
Tip I	Protons	Glass	-	Ge	DTG Excimer laser	15000	-3 -14	[25]
Tip II							206 - 359	
Tip I							10 - 334	
Tip I	Protons	Glass	-	Ge	DTG Excimer laser	100	30 -70	[26]
Tip I								
Tip I	X-Rays	Glass	None	Ge **High content**	Laser UV Hydrogen treatment	500	~ 230	[23]
	Electrons						~ 155	
	X-Rays					10	~ 40	
	Protons						~ 25	
	X-Rays			Low Ge Content	UV Laser hydrogen treatment	500	~ 200	
	Electrons						~ 190	
	X-Rays					10	~ 30	
	Protons						~ 15	
	X-Rays			Ge, B	Laser UV	10	~ 16	
	Protons						~ 12.5	
	X-Rays					500	~ 50	
	Electrons						~ 250	
	X-Rays			P, Ce	UV Laser hydrogen	10	~ 11	
	Protons						~ 4	

	X-Rays				treatment	500	~ 170	
	Electrons						~ 60	
Type	Protons	Glass	-	Ge	Laser UV	0.472	± 40	[27]
Type					Laser FS			
Type				-				
Type	Neutrons	Glass	-	Ge	Laser UV		No changes	
Type					Laser FS			
Type				-				
Type	Neutrons and gamma	Glass	-	F	Laser FS	$5*10^{19}$ n/cm^2	~ 40	[28]
-	Neutrons and gamma	Glass	-	Ge (5%)	-	$5*10^{19}$ n/cm^2 gamma $2*10^6$	< 1.5	[29]
				Ge (20%)				
				Ge, B SMF-28				
-	Electrons	Glass	-	Ge SMF-28	FBG* Interferometrie Laser FS	8	180	[22]

CHAPTER 4. OWN CONTRIBUTIONS IN THE FIELD OF IONIZING RADIATION INTERACTION WITH FIBER OPTIC SENSORS

4.1 LABORATORY-LEVEL CHARACTERIZATION OF OPTICAL COMPONENTS

Own contributions regarding the study of optical fibers and fiber optic sensors in various radiation fields originate from the Optical Fiber Laboratory at CETAL, INFLPR. This laboratory is equipped with a rich infrastructure of devices for testing and characterizing optical fibers and fiber optic sensors, using investigation techniques in transmission or reflection.

4.1.1 Laboratory Characterization and Calibration Infrastructure

The laboratory possesses multiple devices for investigating optical fibers and fiber optic sensors, devices that can operate independently or in combination, providing various useful information about the tested and characterized samples.
The available optical interrogators have the following specifications:
Table 3. Presentation of the main characteristics of the optical interrogators used, highlighting (in green) the main advantages each one offers.

Main characteristics	Micron Optics	Ibsen Photonics	Femto Sensing
Spectral range [nm]	1510-1590	1510-1595	1528-1568
Spectral resolution [pm]	1	5	10
Acquisition frequency [Hz]	1	3000	1000
Number of channels	4	1	4
Dynamic range [dB]	50	15	25
Integrated light source	YES	NO	YES
Compact size	YES	YES	YES
Total advantages	6	3	2

For the spectral characterization of fiber optic sensors, an optical reflectometer produced by LUNA Inc. (U.S.A), model OBR 4600, is also used, with a spectral range between 1525 and 1610 nm. Additionally, for spectral characterization within the laboratory, there are two spectrum analyzers from different manufacturers but with similar specifications. These stand out due to their ability to read a wide spectral range, in this case between 600 and 1750 nm.

Besides the basic equipment used for sensor interrogation, the laboratory also houses complementary devices such as: the Easy Splicer PRO fiber splicer, the Thorlabs FS201 microscope for fiber optic connectors, the Memmert UM 400 oven which aids in temperature calibration of the sensors, cleaning kits for connectors, and various connection fibers and connectors of different lengths.

4.2 OWN CONTRIBUTIONS TO THE EXPERIMENTAL AND THEORETICAL DEVELOPMENT OF THE RESEARCH

With the help of colleagues from the Photonic Investigations Laboratory at CETAL, INFLPR, as well as internal and external collaborators, a series of scientific papers have been published in various specialized journals. Both articles with impact factors and “Proceedings” papers have been published. Below, a few representative articles will be presented, and the results obtained will be discussed.

4.2.1 New Methods and Setups for the Characterization of Fiber Optic Sensors Placed in a Gamma Radiation Field

The series of scientific papers in which I was directly involved, aimed at studying the interaction of various types of radiation with optical fibers or fiber optic sensors, began in 2020 with the paper "A New Setup for Real-Time Investigations of Optical Fiber Sensors Subjected to Gamma-Rays: Case Study on Long Period Gratings" [30].

The paper reports the implementation of a new experimental setup for real-time investigation of optical fibers and fiber optic sensors during exposure to a gamma source. Compared to previous studies, this configuration has several major advantages, such as increased thermal stability, dose rate stability, stability of optical connections, and secure optical path fixation. These advantages lead to higher reproducibility of experiments.

Irradiation took place at IFIN-HH, where two types of gamma irradiators were used. The results obtained from real-time monitoring of radiation effects on fiber optic sensors produced by a research gamma irradiator GC-5000 Co-60 (B.R.I.T., Maharashtra, India) were compared with those obtained using an industrial gamma irradiator SVST Co-60/B (Institute of Isotopes, Budapest, Hungary).

Following the processing and analysis of the data, the following conclusions can be drawn in accordance with the graphs presented below. As can be seen in the two images, the sensor spectra were recorded both before and after irradiation.

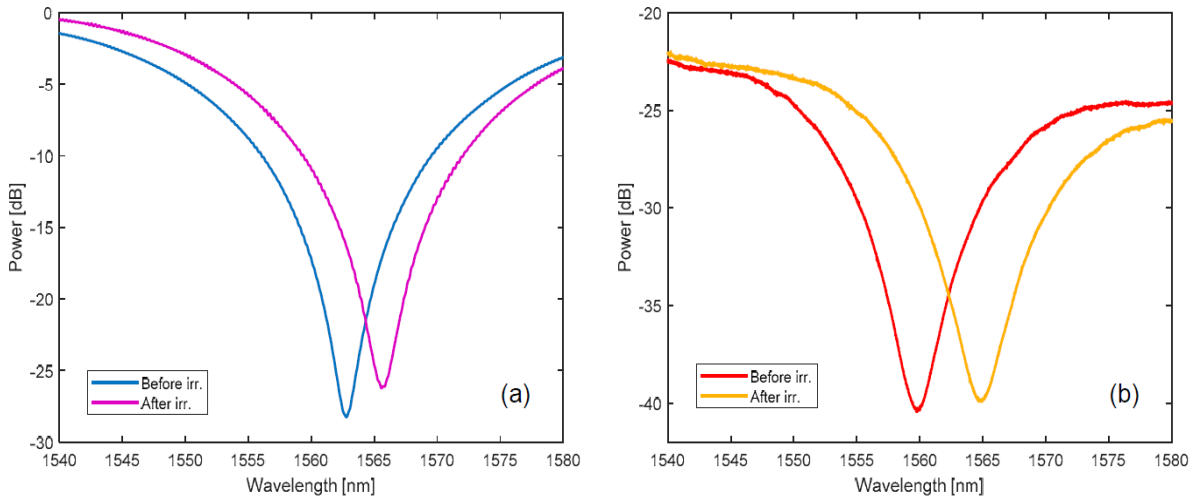


Fig. 3. Comparison of the spectra before and after irradiation: a) For the industrial irradiator SVST Co-60; b) For the research irradiator GC-5000 [30]

In both cases, the central wavelength of the LPG sensors shifted to the right. This is due to the increase in the refractive index of the fiber core during irradiation. For the industrial irradiator, at a total accumulated dose of 35 kGy for the LPG sensors, their wavelength changed by 3.7 nm. The experiment conducted with the research irradiator GC-5000 resulted in a wavelength change of 4.7 nm for a total accumulated sensor dose of 52.6 kGy.

This paper reported the effects of gamma radiation on fiber optic LPG sensors written in standard SMF28 single-mode fiber, using two different setups. The use of a GC-5000 research irradiator for irradiating fiber sensors and monitoring them in real time was a first. This experiment was compared with one conducted in the same period using an industrial SVST

Co-60/B irradiator. Using the same type of LPG sensors, it was observed that the GC-5000 research irradiator is much more suitable for these metrological experiments, offering advantages such as thermal stability, radiation field uniformity, and isolation of the sensors from possible external interferences. These factors support the use of the setup with the research irradiator for activities aimed at studying the effects of radiation on fiber optic sensors through simple and precise control of irradiation parameters.

4.2.2 Study on the effects on FBG-type fiber sensors inscribed using a femtosecond laser, exposed to different types of radiation such as gamma rays and electrons.

The second paper, published in 2021, is "Comparative Study of γ- and e-Radiation-Induced Effects on FBGs Using Different Femtosecond Laser Inscription Methods" [31].

In the experiments conducted for this study, FBG sensors inscribed using two methods, namely PlbPl and PbP with a femtosecond laser, were used. Standard SMF28 fiber was employed, with its core doped with 3% germanium.

Testing of the sensors in a gamma radiation field took place at IFIN-HH using the previously described GC-5000 irradiator. The dose rate was 5.5 kGy/h, and the total accumulated dose for the four FBG sensors was 15 kGy, measured using the classic ethanol-chlorobenzene (ECB) dosimetry system.

For testing the sensors in an electron radiation field, a tunable EEV M5125 linear accelerator was used. The power applied was 2 MW, and the S-band ranged between 2992 and 3001 MHz. The accelerator parameters allowed an equivalent dose rate of 3.2 kGy/min at 60 cm from the accelerator exit window. The dose was verified using a calibrated calorimeter, and the total accumulated dose for the sensors was 15 kGy.

After analyzing the data, the results were compared, leading to the following conclusions:

For the sensor inscribed using the PlbPl method, the wavelength shifted by 60 pm, compared to the sensor inscribed using the PbP method, which shifted its central wavelength by only 6 pm. The FBG-PbP sensor experienced a decrease in the coupling coefficient (k) and the reflection index, whereas for the FBG-PlbPl sensor, these two characteristics increased.

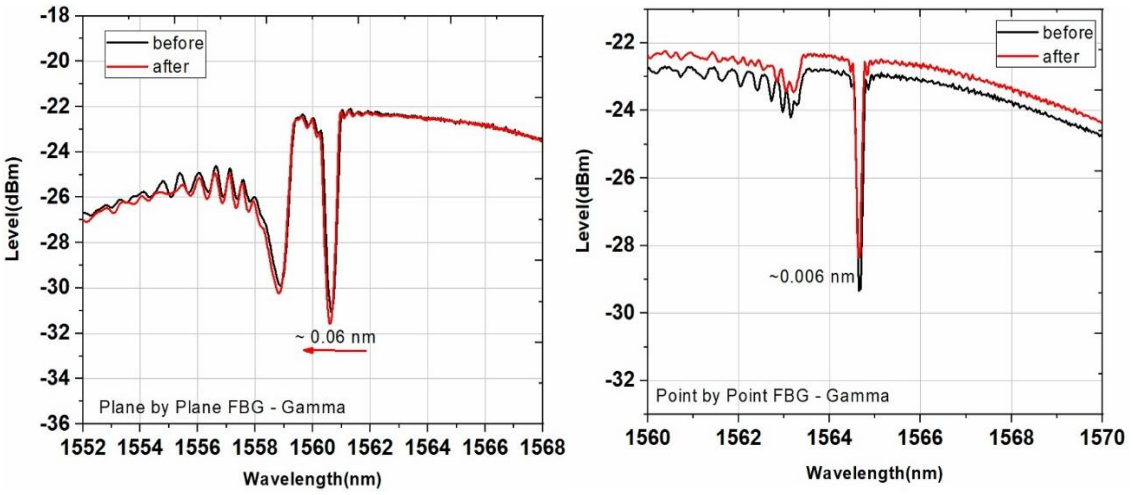


Fig. 4. Presentation of the spectra before and after exposing the FBG sensors to gamma radiation; on the left, the PlbPl inscription method was used, and on the right, the PbP method [31].

Sensors with similar characteristics were also tested in an electron radiation field, and they behaved similarly to exposure to gamma radiation. It is worth noting that the FBG-PbP sensor experienced a much larger change in central wavelength of 224 pm, compared to the FBG-PlbPl sensor, which changed its wavelength by only 52 pm. The behavior of these sensors exposed to electron radiation can be seen in Figure 5, which presents their spectra.

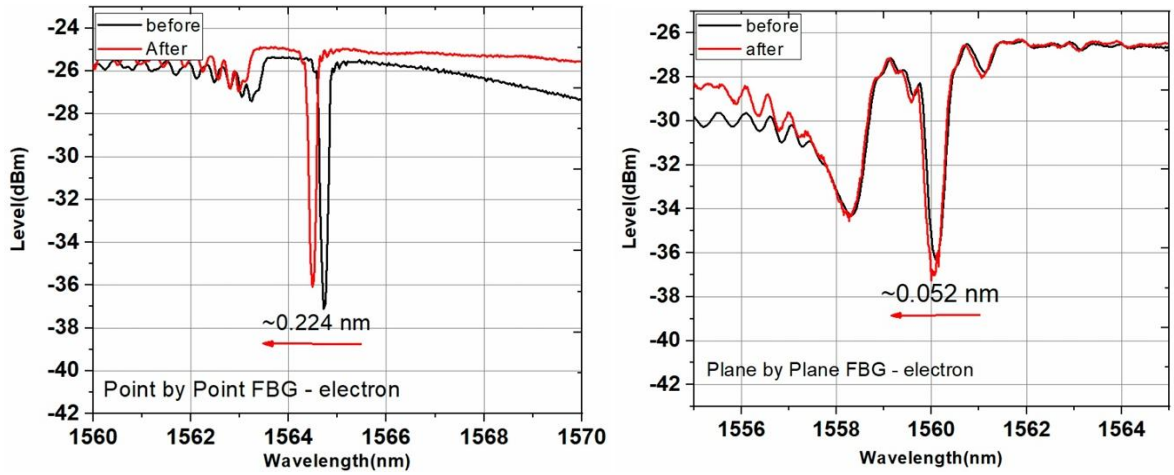


Fig. 5. Presentation of the spectra before and after exposing the FBG sensors to the electron radiation field; on the left, the PbP inscription method was used, and on the right, the PlbPl method [31].

Following the examination of the data and the graphs presented above, upon exposure of the sensors to gamma radiation, a slight increase in the thermal coefficient can be observed for the sensor inscribed using the PlbPl method, from 10.22 pm/°C to 10.45 pm/°C, while the sensor inscribed using the PbP method maintained the same thermal coefficient. When the sensors were exposed to an electron beam, the thermal coefficient changed for both sensors. The sensors written using the PlbPl method showed an increase of 9.19% in the thermal coefficient, while those inscribed using the PbP method increased by 12.91%. After these tests, FTIR investigations were also carried out, which can be found in paper [31].

The above-mentioned paper was the first to address the effect of two types of ionizing radiation (gamma and electrons) on FBG sensors inscribed using two different methods (PbP and PlbPl).

4.2.3 Study on the impact of gamma radiation on LPG-type sensors.

The third scientific paper published within the Doctorate is titled "The Impact of Gamma Irradiation on Optical Fibers Identified Using Long Period Gratings." The authors of this paper studied the effect of gamma radiation on fiber optic LPG sensors in doped fibers.

The sensors used in this experiment were inscribed in different optical fibers (SMF28, VHS100, Draka, BGe, PSM), with either doped or standard cores.

The experiment was divided into two stages: recording the sensor response in real time during exposure to gamma radiation, and verifying the temperature coefficient post-irradiation. The sensors were exposed to the gamma source for a total of 20 hours, with a total accumulated dose of 52 kGy (60 kGy in the case of the Draka sensor).

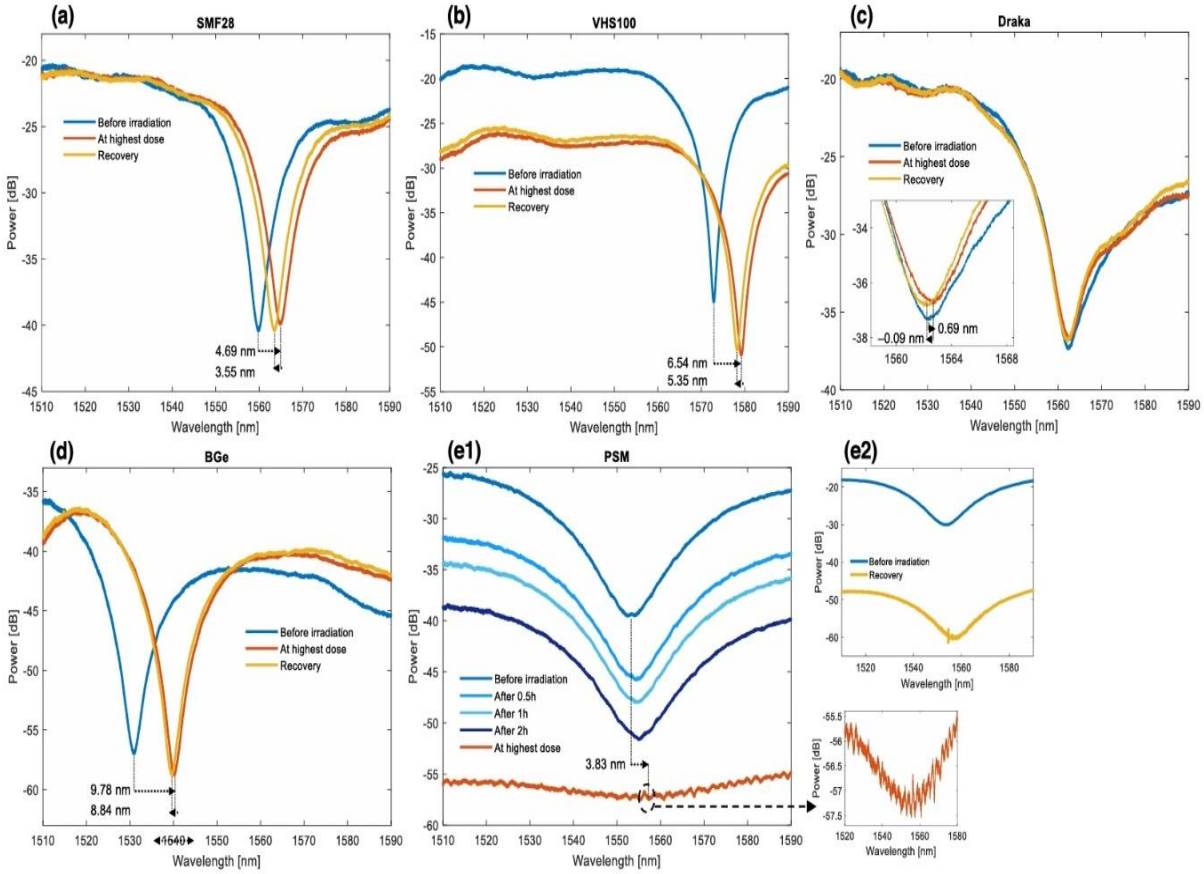


Fig. 6. Spectral response of the LPG sensors before irradiation, at the highest accumulated dose, and after 48 hours of recovery: a) SMF28, b) VHS100, c) Draka, d) BGe. e1) Using the SM125 interrogator, e2) Using the FS22 interrogator [32].

A general characteristic of the sensors during irradiation is that they shift their central wavelength.

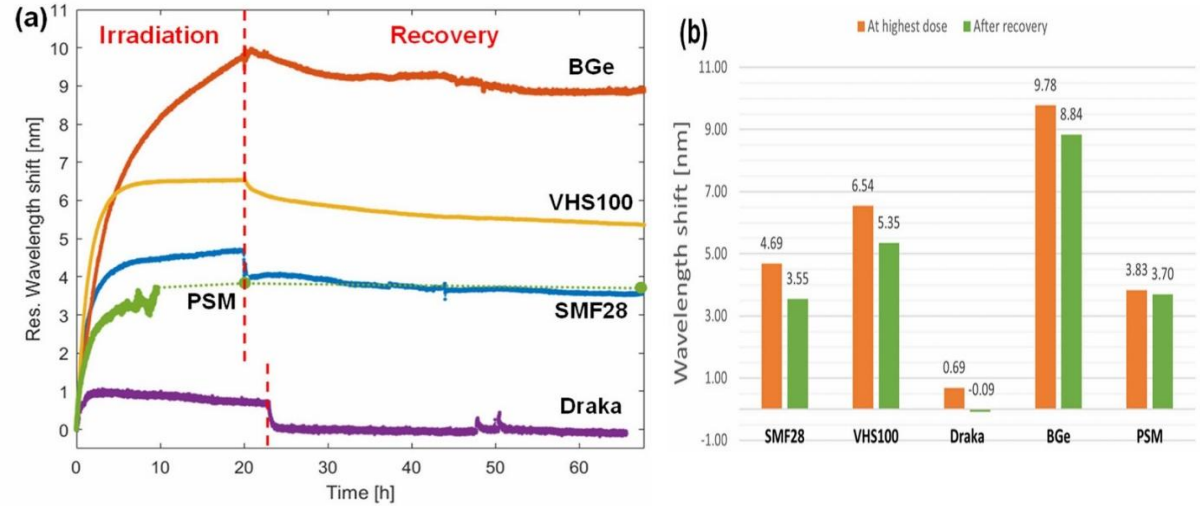


Fig. 7. a) Monitoring the central wavelength of each LPG sensor during irradiation and throughout their recovery period. b) Change in the wavelength of each sensor at the maximum total accumulated dose and after the equivalent 48-hour recovery period [32].

After a period of 48 hours following the removal of the sensors from the radiation field, a slight tendency to return toward the initial wavelength of the sensors can be observed. Temperature sensitivity verification was carried out by calibrating the sensors before exposure to the gamma radiation field.

Discussion and Conclusions:

Upon exposing the sensors to high radiation doses at high dose rates, it was observed that the sensors quickly reach a saturation threshold. Additionally, sensor recovery is influenced by the type of fiber used. For SMF28 and VHS100 fibers, a 20–25% recovery of the wavelength toward the initial value was observed two days after irradiation, whereas for the sensor inscribed in Draka fiber, recovery occurred within only a few hours.

The radiation sensitivity of the sensors ranged between 4 and 10 nm, with the highest recorded for BGe LPG sensors at 9.78 nm, and the lowest recorded for LPG sensors inscribed in Draka fiber.

4.2.4 Investigation of the interaction of radiation with plastic fibers

A fourth paper published in the field of optical fibers used in radiation environments is titled "Influence of gamma and electron radiation on perfluorinated optical fiber material composition" [33]. This study aimed to investigate the materials of a special optical fiber type from Chromis Fiberoptics Inc. (CYPTO) and their behavior when exposed to different types of radiation. In this case, the materials composing the fiber were analyzed using FTIR and RAMAN spectroscopy methods.

For gamma radiation exposure, a gamma-chamber source was used. For electron beam exposure, a linear electron accelerator from the Accelerators Laboratory at INFLPR was used. The dose rate for electron irradiation was 3.2 kGy/min, and the fibers were positioned 60 cm from the accelerator exit flange.

After exposing the fibers to the two types of radiation, FTIR analysis was performed for each irradiated sample to check for possible changes in the material.

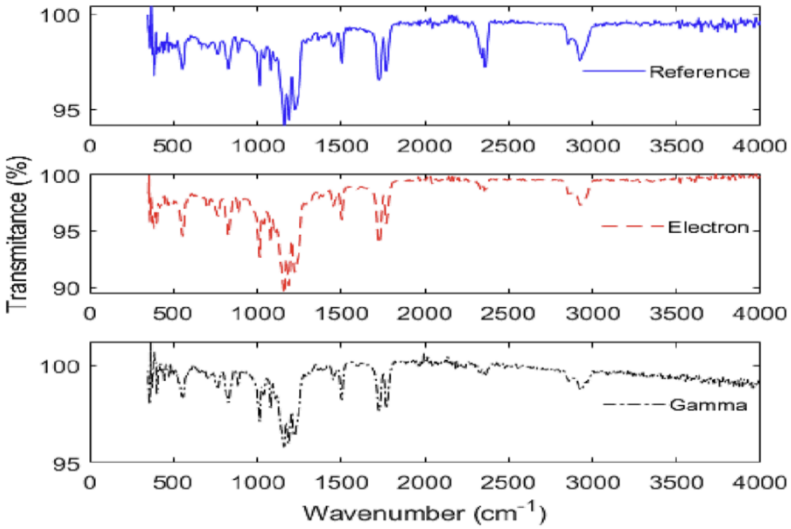


Fig. 8. Spectral analysis of fibers using FTIR

As observed from the FTIR analyses, the largest difference between irradiated and non-irradiated fibers is in the optical fiber transmission, which changed by 10% for the fiber exposed to the electron beam. Following the FTIR analyses, RAMAN analyses were also conducted to confirm the previous results.Comparing the two methods for investigating irradiated and non-irradiated fibers, it can be seen that the recorded spectra show higher intensities around the same values (700, 1470, 1656 cm^{-1}). The greatest differences between samples are observed in the 400–600 cm^{-1} region. For the samples exposed to gamma radiation and the reference (non-irradiated) samples, the spectra are similar, whereas for the samples exposed to electrons, a considerable difference in intensity can be observed, with much lower values. At the same time, in the 2900–3200 cm^{-1} region, the greatest differences between the samples can be observed.

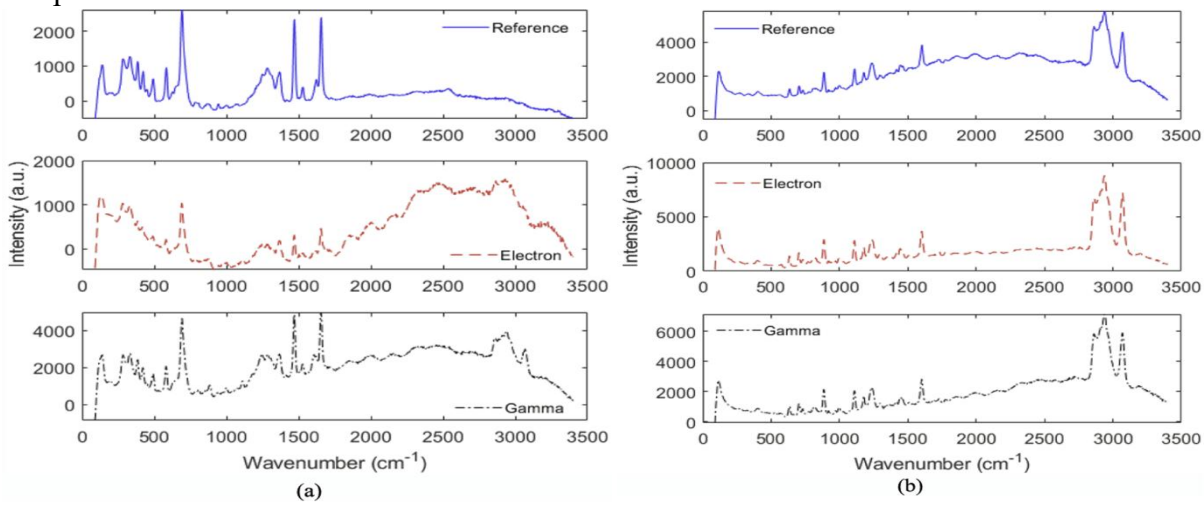


Fig. 9. Analysis of optical fibers using RAMAN: a) Core analysis b) Analysis of the coatings attached to the cladding

In conclusion, the following points can be drawn from this study:

In the case of electron irradiation, the optical fiber undergoes greater changes than those caused by exposure to gamma radiation. Comparing the two types of radiation in the obtained RAMAN spectra, the largest variations can be observed around 1500 cm^{-1}. Additionally, for both irradiations, molecular changes in the CYTOP fiber can be seen through the appearance of CH_3 groups. These changes lead to altered interactions between the fiber core and cladding. The absorption of the materials composing the fiber increased, resulting in decreased transmission.

4.2.5 Evaluation of the effects of different types of radiation on radiation-resistant fibers

The fifth paper, which aimed to investigate fiber optic sensors in a radiation field, is titled "Comparative evaluation of electron and gamma induced effects on FBG fabricated in standard and radiation-hardened optical fibers by different techniques" [34]. This study examined the effects on four FBG sensors placed in an electron field and a gamma radiation field.

For this experiment, two fibers were used, each with two sensors inscribed using a phase mask during continuous UV exposure. The fibers were germanium-doped, and the UV exposure covered a length of 10 cm. In the other two fibers, the sensors were inscribed using a femtosecond pulsed laser, produced by Loptek GmbH (Berlin, Germany). The optical fiber used was a commercial single-mode model FIBERCORE SM1500SC.

Three experimental setups were used for this study:

The first setup was used for calibrating the four sensors with temperature in the Optical Fiber Laboratory at INFLPR – CETAL.

The second setup was carried out at the IRASM department, part of IFIN-HH, using the GC-5000 research irradiator, described in detail in paper [30].

The third experimental setup was performed in the Accelerators Laboratory at INFLPR, with a tunable EEV M5125 linear accelerator as the radiation source.

To draw correct conclusions about the two radiation experiments, several observations must be made. Although the exposure time was the same for both types of radiation, the total accumulated dose differs. Additionally, the electron energy is different from that of the gamma radiation. A clearer picture can be seen in Fig. 10:

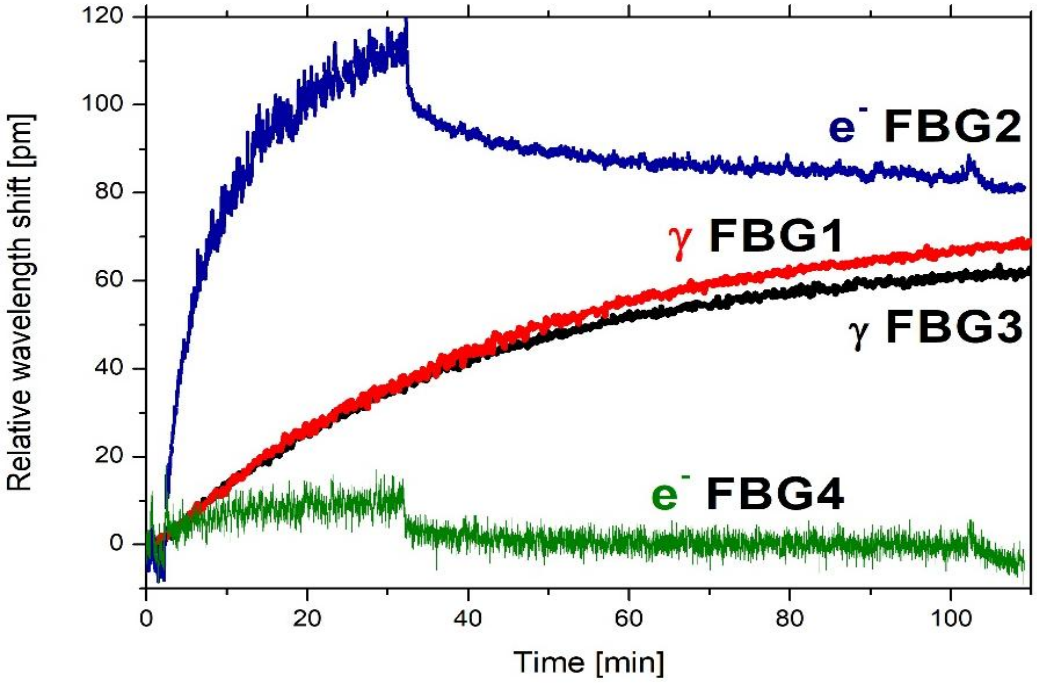


Fig. 10. Change in the Bragg wavelength of the four sensors present in the two irradiation experiments [34]

The BWS change occurs exclusively due to the effects experienced by the sensors during interaction with radiation, as the thermal effect was removed from the recorded data. This can be more easily observed in Table 10, which presents the fiber type, fabrication method, and the behavior of each sensor during each irradiation session.

Table 4. Results of the irradiation of the four sensors [34].

Sensor No.	Fiber type	Fabrication method	Radiation type	Accumulated dose	Dose rate	BWS
FBG1	Ge-doped	Phase-mask	Gamma	56 kGy	2,45kGy/h	40pm
FBG2	Ge-doped	Phase-mask	Electrons	120 kGy	228kGy/h	120pm
FBG3	Pure silica	Fs-laser	Gamma	56 kGy	2,45kGy/h	10pm
FBG4	Pure silica	Fs-laser	electrons	120 kGy	228kGy/h	10 pm

Following temperature calibration of the sensors in the laboratory, their sensitivity is 10 pm/°C. While thermal effect compensation was possible for the data obtained from exposure to gamma radiation, the same cannot be said for electron radiation exposure. Compensating for the thermal effect in the case of electron radiation would render the data inconsistent, as the temperature increased by approximately 4 °C, leading to an expected BWS change of about 40 pm for each sensor according to laboratory calibrations. While it is possible to reduce this effect for sensor FBG2, it is not possible for sensor FBG4. The data collected during irradiation suggest that sensor FBG4 may experience a negative wavelength shift, which produces a natural temperature compensation; further investigations are required.

4.2.6 Effects of gamma radiation on LPG sensors and on the thin films deposited over them

Within a consortium created with experts from Italy, Poland, and Romania, the effects of radiation on LPG fiber optic sensors customized with thin-film coatings were studied.

For the experiments, LPG sensors were fabricated in standard Nufern (USA) S1310 optical fibers, customized to withstand harsh environments. After sensor inscription, the coatings were deposited on the fibers. First, polystyrene (PS) 10% in chloroform was applied using a dip-coating process, moving the fiber through the solution at a speed of 30 mm/min. Metal oxides Al_2O_3, TiO_2, and Ta_2O_5 films were also deposited using atomic layer deposition (ALD) with the Veeco Savannah S100 system, which enhanced coating uniformity. After the coatings were applied, the central wavelength of the LPG sensor shifted by 10 nm.

For sensor irradiation, the setup described in paper [30] was used, employing a GC-5000 irradiator from BRIT, India. A special metal holder was constructed to keep the fiber taut throughout the irradiation. The dose rate was 2.3 kGy/h, and the sensors were exposed for a total of 20 hours. At the end of each irradiation, the sensors were observed for 5 hours to monitor any potential recovery. As a reference, an uncoated LPG sensor was irradiated under the same experimental conditions.

During irradiation, the sensor spectra were recorded in real time by the optical interrogator, and the data are presented in Figure 11.

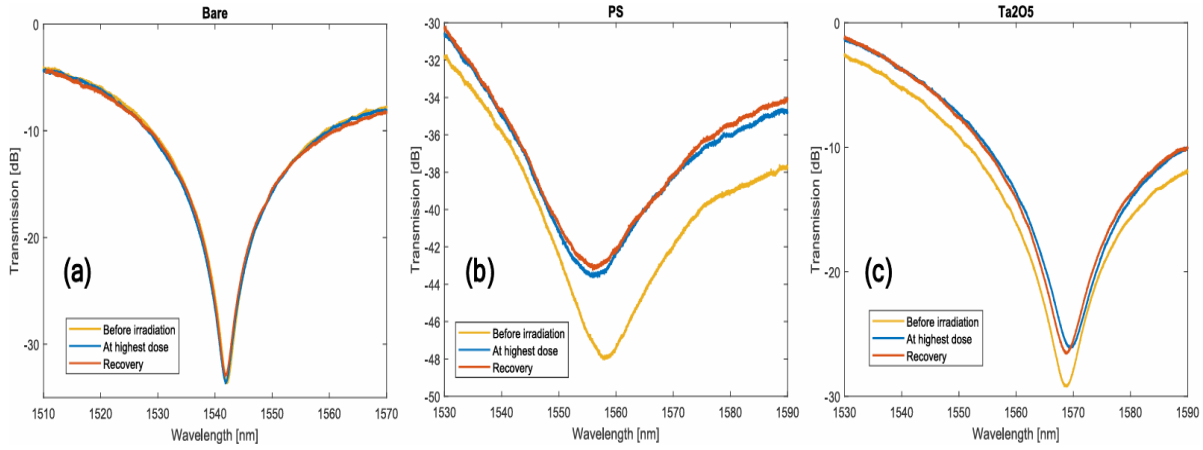


Fig. 11. Effects of gamma radiation on sensors: a) Simple LPG sensor b) LPG – PS c) LPG - Ta_2O_5 [35]

As observed in Figure 11a, the simple LPG sensor shifts its central wavelength 0.40 nm to the right, and this change is permanent. In the case of LPG-PS (Figure 11b), a wavelength shift of 2.51 nm is observed at the moment of reaching the maximum irradiation threshold, with a slight tendency to recover after removal from the irradiation zone. For the LPG-PS sensor, an increase in signal attenuation can also be observed, although it is not significant enough to compromise the experiment or sensor readout. The LPG-Ta_2O_5 sensor also shows changes in central wavelength, but in this case, it shifts 0.51 nm to the left. After irradiation stops, the sensor exhibits full recovery of its wavelength to the initial value.

As a brief remark, comparing the sensors clearly shows that the coatings influence their response to gamma radiation.

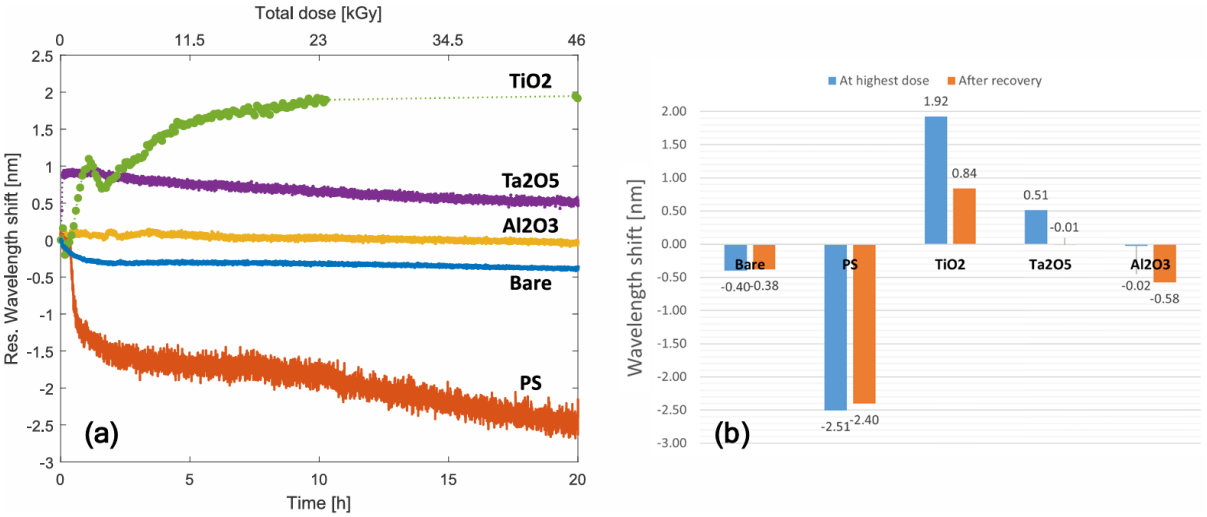


Fig. 12. Change in central wavelengths following exposure of the sensors to gamma radiation: a) Real-time data acquisition b) Monitoring wavelength recovery after exposure [35]

Figure 12 presents the wavelength values of each sensor at the point of maximum radiation dose and after the recovery period.

As expected from previous experiments, the LPG sensor inscribed in fibers with a pure silica core and a fluorine-doped cladding is radiation-resistant, showing only minor Bragg wavelength changes due to the fluorine doping. For LPGs coated with Al_2O_3 and PS, a slight blue-shift tendency of the wavelength is observed, equivalent to 0.58 nm and -2.51 nm, respectively. The other two sensors coated with Ta_2O_5 and TiO_2 show wavelength shifts to the left of 0.51 nm and 1.92 nm.

This study aimed to investigate the effects of ionizing radiation on LPG sensors with different coatings. The general conclusion is that, depending on the coatings applied, the sensors reacted differently to prolonged radiation exposure.

4.2.7 Impact of a beam of accelerated electrons on LPG sensors fabricated in different fibers

The most recent paper published on the exposure of fiber optic sensors in a radiation field is titled “Electron Radiation Impact on Long Period Gratings in Different Optical Fibers.” The authors proposed exposing LPG sensors to an electron field to study the induced effects. For the first time in the literature, the results of the interaction between LPG sensors and radiation emitted by an electron beam were reported.

For the experiments, four LPG sensors were fabricated in different fibers. Table 11 identifies the fibers in which the sensors were inscribed, the core composition (dopants present), the cladding composition, the designation for each sensor, and the period of the structures created.

Table 5. Characteristics of the four LPG sensors [36]

Fiber model	Core composition	Cladding composition	LPG id	LPG period Λ
Corning SMF28	Ge-doped	Pure-silica	SMF	395 μm
Fibercore PS1250/1500	B/Ge co-doped	Pure-silica	BGe	300 μm
Nufern S1310	Pure-silica	F-doped	Pure-silica	440 μm
FORC P-SM-5	P-doped	P-doped	P-doped	395 μm

In this experiment, a tunable EEV M5125 linear accelerator with a power of 2 MW and a frequency band between 2992–3001 MHz was used. The dose rate was 6 kGy/min, with a total accumulated dose of 192 kGy.

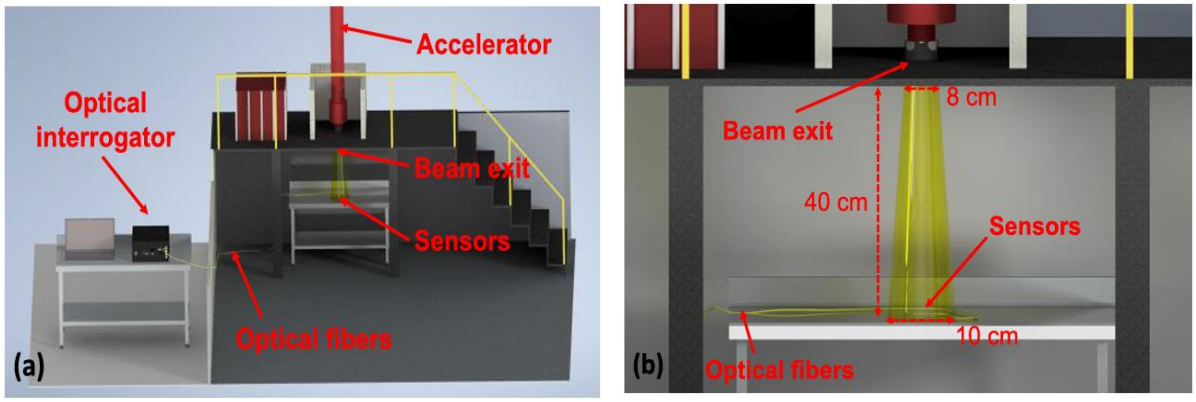


Fig. 13. Schematic presentation of the experimental setup a) overview b) detailed view of the interaction area [36].

The experimental area is divided into two sections: the interaction zone, where the sensors were placed in the electron beam at a distance of 40 cm from the accelerator's outer flange, and the control zone, which contains both the accelerator monitoring equipment and the sensor interrogation systems, located in a separate and shielded area from the experimental zone.

The experiment was divided into three phases. The first two involved exposing the sensors to two similar doses of 6 kGy each. These initial steps were carried out to test the reproducibility of the experiment and to assess the sensitivity of each individual sensor. The third phase of the experiment involved prolonged exposure of the sensors to a total accumulated dose of 180 kGy. This phase aimed to test the operational limits of the sensors. In total, the sensors were exposed for 52 minutes, accumulating a total dose of 192 kGy. As can be seen in the following image, the most sensitive sensor to electron radiation is the one inscribed in the B-Ge doped fiber, while the most resistant sensor to this type of radiation is the one inscribed in the high-purity silica fiber.

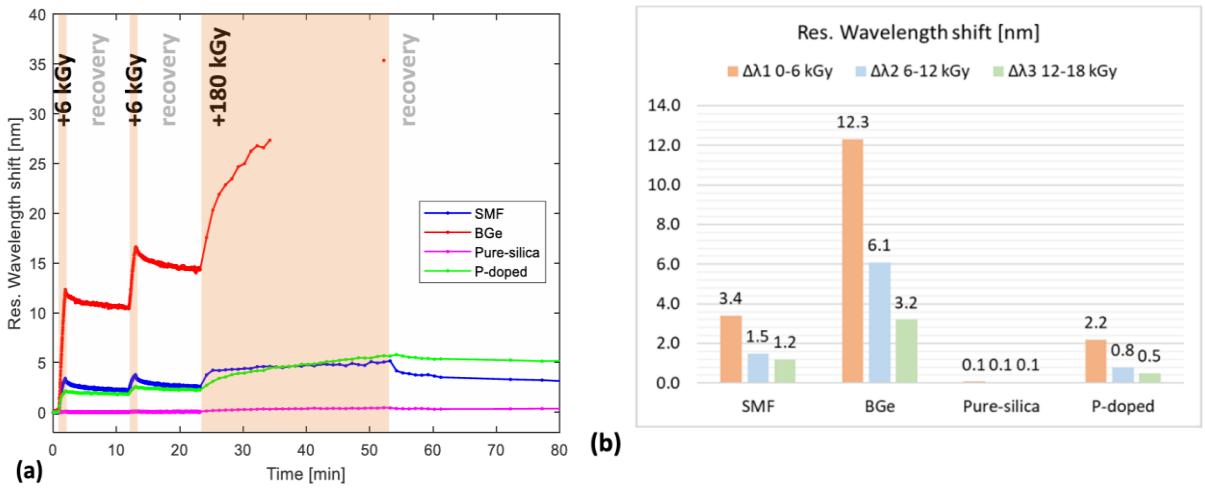


Fig. 14. Shift in the central wavelength of each sensor during irradiation, b) Wavelength shift of the LPG sensors for each irradiation phase, starting from the previously accumulated dose [36].

In Figure 14, the three irradiation phases (highlighted in orange) can be observed, as well as the recovery phases of the sensors over an 80-minute monitoring period. As shown in the image, all sensors exhibit a wavelength shift to the right and a slight return toward their initial wavelength during the irradiation breaks. Another observation that can be made is that the sensors tend to stabilize after a continuous exposure period of 30 minutes.

Tabel 6. Central wavelength shift of each sensor during all three irradiation stages, in picometers [36].

LPG id	S_1 0-6 kGy [pm/kGy]	S_2 6-12 kGy [pm/kGy]	S_3 12-18 kGy [pm/kGy]
SMF	570	257	198
BGe	2057	1015	533
P-doped	358	128	77

Following data processing, a decrease in sensor sensitivity was observed with each irradiation stage. From stage 1 (0–6 kGy) to stage 3 (12–18 kGy), their sensitivity dropped by 65% to 80%, depending on the type of fiber in which they were inscribed. Another noteworthy observation is that the sensor fabricated in the B-Ge doped fiber can detect a minimum dose of 0.5 Gy, whereas the sensor inscribed in SMF and the one in the P-doped fiber can detect radiation starting from 2 Gy and 3 Gy, respectively.

The long-term effects of radiation on the fiber are also a topic of interest addressed in this study. The sensors were analyzed at various time intervals — 21 hours, 8 days, 6 months, and 12 months after irradiation. After analyzing the spectra, it was observed that the recovery of the sensors began immediately after they were removed from the irradiation area. The recovery was gradual and stabilized after 6 months from the initial exposure to radiation.

To further understand the fiber's recovery effects, the Bragg central wavelength of the sensors was also monitored.

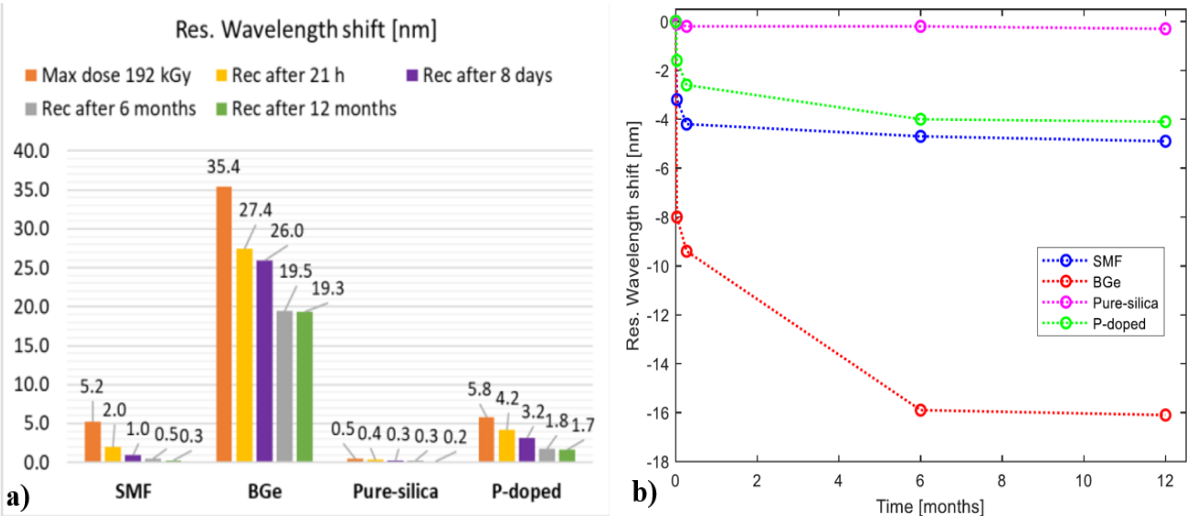


Fig. 15. Monitoring of the Bragg wavelength of the sensors and its variation. a) Monitoring of the wavelength shift of the sensors before irradiation, after accumulating 192 kGy, and post-irradiation at different time intervals (21 hours, 8 days, 6 months, 12 months). b) Wavelength shift after removing the sensors from the irradiation area over a period of 12 months [36].

Following these periodic inspections of the fibers, it was observed that none of the LPG sensors fully returned to their initial values prior to irradiation. The greatest recovery was seen in the sensors inscribed in SMF fiber and in the Nufern high-purity silica fiber, which were only 0.3 nm and 0.2 nm, respectively, from their original pre-irradiation values. In the case of the sensors inscribed in B-Ge and P-doped fibers, a significant shift in the Bragg wavelength was still present even 12 months after irradiation. Although a recovery trend can be observed, it decreases considerably after the first 6 months, and the structural changes in the fiber appear to be permanent, with only about 45% recovery of the initial value.

In conclusion, this work reports for the first time the effects of accelerated electron radiation on LPG-type sensors. Sensors inscribed in four different fibers with varying compositions were studied. Additionally, the recovery behavior of the fibers was analyzed after their removal from the irradiation area over a period of one year. The fibers were exposed to a total accumulated dose of nearly 200 kGy, and the sensors' responses varied depending on the fiber in which they were inscribed.

CHAPTER 5. CONCLUSIONS

5.1 General Conclusions

The early stage of optical sensors, optical fibers, and fiber optic sensors:

This work aimed to present the usefulness of fiber optic sensors used in multiple fields, with an emphasis on sensors employed in ionizing radiation environments. As previously mentioned in Chapter 1, optical sensors began to take shape more than two centuries ago. In the early days of optical sensors, they were primarily used for transmitting messages over long distances using

light. In 1854, the first experiment demonstrated that light could be guided using a stream of water. The phenomenon of light guiding attracted significant attention from many researchers in the following years, which eventually led to the creation of optical fibers in the mid-20th century. These early steps laid the foundation for today's information transmission systems, which rely on optical fibers for approximately 90% of data transfer.

The first use of optical fibers as sensors took place in 1970, employing two fiber bundles—one as a transmitter and the other as a receiver. These two fibers were used to measure the distance to an object by reflecting a light beam from one fiber and capturing it with the other. Considering the rapid technological advancements in this field, fiber optic sensors gradually began to be used for detecting various physical quantities such as temperature, humidity, distance, displacement, pressure, and more.

The main reasons fiber optic sensors have attracted significant interest for use in various industries are: reduction of production costs through the maturation of manufacturing technologies, increased sensitivity and accuracy for applications where they are already used, development of new sensors through different technologies for novel applications across various fields, their small size, the ability to functionalize them, the long distances they can cover, the large monitoring range, and their resistance in harsh environments.

Fiber optic sensors used in ionizing radiation fields.

In this work, the focus was directed towards the interaction of fiber optic sensors with various ionizing radiation fields. The manufacturing parameters chosen for producing the fibers and fiber optic sensors directly influence how they respond to ionizing radiation environments. Equally important is the selection of materials used to dope the optical fiber in order to achieve the desired response from the sensors employed in different experiments. Considering that most fiber optic sensors use Bragg-type gratings, the majority of experiments involve FBG and LPG sensors. For a clear classification, the effects of ionizing radiation on fiber optic sensors were addressed separately depending on the type of ionizing radiation.

5.2 Conclusions and Own Contributions

In the case of sensors inscribed in doped optical fibers, it can be observed that they have increased sensitivity to different types of radiation. The sensor response can vary depending on the specific dopant as well as its concentration in the fiber. The Bragg wavelength can shift by tens of nanometers in the case of ultra-sensitive radiation sensors, making it possible to use them as radiation detectors. The major advantage for which this type of sensor could be used in the future for monitoring and diagnosing radiation fields lies in the fact that the spectral response of the sensors can be recorded and interpreted in real time, providing important information about environmental parameters or radiation field parameters during irradiation stages.

Within the current PhD thesis, I have reported experiments conducted during the doctoral studies involving FBG/LPG-type optical fiber sensors exposed to gamma and electron ionizing radiation, documented in 10 scientific papers. The research topics were original and

subsequently published in high-impact scientific journals (Q1 quartile), forming the foundation for my future scientific career in experimental research within the fields of optics, photonics, and ionizing radiation.

My personal contributions to these scientific works can be summarized as follows:

Implementation of procedures for irradiation experiments with ionizing radiation on photonic devices based on optical fibers.

CAD design of experimental setups to be used in relevant scientific reports.

Fabrication of opto-mechanical components necessary for customized experimental setups tailored to specific applications.

Implementation of experimental setups in the laboratory and in adjacent infrastructures. Data acquisition and processing throughout the experimental stages. Theoretical studies involving the effects of ionizing radiation on optical fibers, dopant materials, Bragg grating structures, and correlating these effects with fabrication models of fiber optic sensors to optimize devices for security applications in harsh environments.

5.3 FUTURE RESEARCH DIRECTIONS

The importance of optical fibers and fiber optic sensors is clear for technological advancement in various key fields worldwide. The increasingly widespread communication networks and fiber optic sensors found in more and more applications amplify the need for research in this domain.

Together with the team at the Laboratory, I will focus on activities such as:

Developing fiber optic sensors with high sensitivities for medical applications, such as localized detection of radiation dose during radiotherapy procedures.

Developing new experimental setups to improve data quality and eliminate current limitations by minimizing device handling through automation, increasing the number of sensors monitored in parallel, and real-time processing of spectral responses correlated with ionizing radiation.

Theoretical studies on addressing mixed fields of ionizing radiation generated by laser-matter interactions and implementing fiber optic platforms in such fields.

Using optical fibers in biomedical and biosensing applications.

Theoretical studies and experimental development of complementary methods for detecting ionizing radiation through multimode optical fibers, scintillation phenomena, and photonic particle detectors for complex monitoring solutions.

CHAPTER 6. REFERENCES

[1] J. Tyndall, *Notes of a course of nine lectures on light delivered at the Royal institution of Great Britain April 8-June 3, 1869* . 1820.

[2] A. G. Bell, "On the production and reproduction of sound by light," *Am J Sci*, vol. s3-20, no. 118, pp. 305–324, Oct. 1880, doi: 10.2475/AJS.S3-20.118.305.

[3] Casimer. DeCusatis, "Fiber optic data communication : technological trends and advances," p. 568, 2002, Accessed: Jun. 29, 2023. [Online]. Available: https://books.google.com/books/about/Fiber_Optic_Data_Communication.html?hl=ro&id=yDjUlE8VTLsC

[4] C. P. Sandbank, "FIBRE OPTIC COMMUNICATION SYSTEMS.," pp. 3–12, 1977, doi: 10.1109/EUMA.1977.332387.

[5] G. Rademacher *et al.*, "Randomly Coupled 19-Core Multi-Core Fiber with Standard Cladding Diameter," *Optical Fiber Communication Conference (OFC) 2023 (2023), paper Th4A.4*, p. Th4A.4, Mar. 2023, doi: 10.1364/OFC.2023.TH4A.4.

[6] K. O. Hill, Y. Fujii, D. C. Johnson, and B. S. Kawasaki, "Photosensitivity in optical fiber waveguides: Application to reflection filter fabrication," *Appl Phys Lett*, vol. 32, no. 10, pp. 647–649, May 1978, doi: 10.1063/1.89881.

[7] K. O. Hill and G. Meltz, "Fiber Bragg grating technology fundamentals and overview," *Journal of Lightwave Technology*, vol. 15, no. 8, pp. 1263–1276, Aug. 1997, doi: 10.1109/50.618320.

[8] S. K. Hoeffgen *et al.*, "Comparison of the radiation sensitivity of fiber bragg gratings made by four different manufacturers," *IEEE Trans Nucl Sci*, vol. 58, no. 3 PART 2, pp. 906–909, Jun. 2011, doi: 10.1109/TNS.2011.2106800.

[9] P. Cetier, S. Rougeault, M. Monerie, E. Fertein, and F. Lahoreau, "Behavior of Bragg Gratings, Written in Germanosilicate Fibers, Against ϒ-Ray Exposure at Low Dose Rat," *IEEE Photonics Technology Letters*, vol. 6, no. 11, pp. 1350–1352, 1994, doi: 10.1109/68.334836.

[10] P. Ferdinand *et al.*, "Optical fibre Bragg grating sensors for structure monitoring within the nuclear power plants," *https://doi.org/10.1117/12.198636*, vol. 2425, pp. 11–20, Dec. 1994, doi: 10.1117/12.198636.

[11] A. Gusarov, S. Vasiliev, O. Medvedkov, I. Mckenzie, and F. Berghmans, "Stabilization of fiber bragg gratings against gamma radiation," *Proceedings of the European Conference on Radiation and its Effects on Components and Systems, RADECS*, 2007, doi: 10.1109/RADECS.2007.5205516.

[12] A. Piccolo, S. Delepine-Lesoille, M. Landolt, S. Girard, Y. Ouerdane, and C. Sabatier, "Coupled temperature and γ-radiation effect on silica-based optical fiber strain sensors based on Rayleigh and Brillouin scatterings," *Opt Express*, vol. 27, no. 15, p. 21608, Jul. 2019, doi: 10.1364/OE.27.021608.

[13] F. Esposito *et al.*, "Real-time analysis of arc-induced Long Period Gratings under gamma irradiation," *Sci Rep*, vol. 7, Mar. 2017, doi: 10.1038/SREP43389.

[14] A. I. Gusarov *et al.*, "High total dose radiation effects on temperature sensing fiber Bragg gratings," *IEEE Photonics Technology Letters*, vol. 11, no. 9, pp. 1159–1161, Sep. 1999, doi: 10.1109/68.784237.

[15] A. Morana *et al.*, "Radiation-Hardened Fiber Bragg Grating Based Sensors for Harsh Environments," *IEEE Trans Nucl Sci*, vol. 64, no. 1, pp. 68–73, Jan. 2017, doi: 10.1109/TNS.2016.2621165.

[16] H. Henschel, S. K. Hoeffgen, K. Krebber, J. Kuhnhenn, and U. Weinand, "Influence of fiber composition and grating fabrication on the radiation sensitivity of fiber bragg gratings," *Proceedings of the European Conference on Radiation and its Effects on Components and Systems, RADECS*, 2007, doi: 10.1109/RADECS.2007.5205461.

[17] J. Kuhnhenn *et al.*, "Gamma Radiation Tests of Radiation-Hardened Fiber Bragg Grating-Based Sensors for Radiation Environments," *IEEE Trans Nucl Sci*, vol. 64, no. 8, pp. 2307–2311, Aug. 2017, doi: 10.1109/TNS.2017.2673023.

[18] A. Pal *et al.*, "Sensors for Harsh Environment: Radiation Resistant FBG Sensor System," *Journal of Lightwave Technology*, vol. 35, no. 16, pp. 3393–3398, Aug. 2017, doi: 10.1109/JLT.2016.2598666.

[19] D. G. Sporea, A. Stəncalie, C. D. Neguţ, G. Pilorget, S. Delepine-Lesoille, and L. Lablonde, "Comparative study of long period and fiber Bragg gratings under gamma irradiation," *Sens Actuators A Phys*, vol. 233, pp. 295–301, Aug. 2015, doi: 10.1016/J.SNA.2015.07.007.

[20] K. Kalli *et al.*, "L-band CYTOP Bragg gratings for ultrasound sensing," p. 8, May 2018, doi: 10.1117/12.2307129.

[21] S. Ju, Y. Kim, K. Linganna, Y. H. Kim, and W. T. Han, "Effect of Temperature and Gamma-Ray Irradiation on Optical Characteristics of Fiber Bragg Grating Inscribed Radiation-Resistant Optical Fiber," *Photonic Sensors*, vol. 10, no. 1, pp. 16–33, Mar. 2020, doi: 10.1007/S13320-019-0567-4/METRICS.

[22] D. Sporea, A. Stăncălie, N. Becherescu, M. Becker, and M. Rothhardt, "An electron beam profile instrument based on FBGs," *Sensors (Switzerland)*, vol. 14, no. 9, pp. 15786–15801, Aug. 2014, doi: 10.3390/S140915786.

[23] T. Blanchet *et al.*, "X-Ray, proton, and electron radiation effects on type i fiber bragg gratings," *IEEE Trans Nucl Sci*, vol. 65, no. 8, pp. 1632–1638, Aug. 2018, doi: 10.1109/TNS.2018.2823771.

[24] E. W. Taylor, K. E. Hulick, J. M. Battiato, A. D. Sanchez, J. E. Winter, and A. R. Pirich, "Response of germanium-doped fiber Bragg gratings in radiation environments," *https://doi.org/10.1117/12.354676*, vol. 3714, pp. 106–113, Jul. 1999, doi: 10.1117/12.354676.

[25] E. Currás *et al.*, "Influence of the fiber coating on the proton radiation sensitivity of fiber bragg gratings," *Proceedings of the European Conference on Radiation and its Effects on Components and Systems, RADECS*, pp. 345–348, 2011, doi: 10.1109/RADECS.2011.6131410.

[26] M. FRÃ–VEL *et al.*, "Proton Radiation Sensitivity of Fiber Bragg Gratings for Particle Colliders," *Structural Health Monitoring 2013*, vol. 0, no. 0, 2013, Accessed: Sep. 08, 2025. [Online]. Available: https://www.dpi-proceedings.com/index.php/shm2013/article/view/22811

[27] M. Bakaic *et al.*, "Fiber-optic Bragg gratings for temperature and pressure measurements in isotope production targets for nuclear medicine," *Applied Sciences (Switzerland)*, vol. 10, no. 13, Jul. 2020, doi: 10.3390/APP10134610.

[28] L. Remy, G. Cheymol, A. Gusarov, A. Morana, E. Marin, and S. Girard, "Compaction in optical fibres and fibre Bragg gratings under nuclear reactor high neutron and gamma fluence," *2015 4th International Conference on Advancements in Nuclear Instrumentation Measurement Methods and their Applications, ANIMMA 2015*, 2015, doi: 10.1109/ANIMMA.2015.7465627.

[29] R. S. Fielder, "High Neutron Fluence Survivability Testing of Advanced Fiber Bragg Grating Sensors," pp. 650–657, Feb. 2004, doi: 10.1063/1.1649627.

[30] A. Stancalie *et al.*, "A New Setup for Real-Time Investigations of Optical Fiber Sensors Subjected to Gamma-Rays: Case Study on Long Period Gratings," *Sensors 2020, Vol. 20, Page 4129*, vol. 20, no. 15, p. 4129, Jul. 2020, doi: 10.3390/S20154129.

[31] A. Theodosiou *et al.*, "Comparative Study of γ- and e-Radiation-Induced Effects on FBGs Using Different Femtosecond Laser Inscription Methods," *Sensors 2021, Vol. 21, Page 8379*, vol. 21, no. 24, p. 8379, Dec. 2021, doi: 10.3390/S21248379.

[32] F. Esposito *et al.*, "The Impact of Gamma Irradiation on Optical Fibers Identified Using Long Period Gratings," *Journal of Lightwave Technology*, vol. 41, no. 13, pp. 4389–4396, Jul. 2023, doi: 10.1109/JLT.2022.3191163.

[33] A. Leal-Junior *et al.*, “Influence of gamma and electron radiation on perfluorinated optical fiber material composition,” *Mater Lett*, vol. 340, p. 134205, Jun. 2023, doi: 10.1016/J.MATLET.2023.134205.

[34] R. Mihalcea, D. Ighigeanu, D. Negut, and A. Stancalie, “COMPARATIVE EVALUATION OF ELECTRON AND GAMMA INDUCED EFFECTS ON FBG FABRICATED IN STANDARD AND RADIATION HARDENED OPTICAL FIBERS BY DIFFERENT TECHNIQUES,” *U.P.B. Sci. Bull., Series A*, vol. 85, no. 3, p. 2023.

[35] F. Esposito *et al.*, “Optical properties of thin films monitored in real-time at high gamma radiation doses using long period fiber gratings,” *Opt Laser Technol*, vol. 176, p. 111019, Sep. 2024, doi: 10.1016/J.OPTLASTEC.2024.111019.

[36] A. Stancalie *et al.*, “Electron radiation impact on Long Period Gratings in different optical fibers,” *IEEE Sens J*, 2024, doi: 10.1109/JSEN.2024.3508885.